Exploring the Mechanism for the Synthesis of Silsesquioxanes. 4. The Synthesis of T_8

Takako Kudo* and Kazuya Machida

Department of Fundamental Studies, Faculty of Engineering, Gunma University, Kiryu 376-8515, Japan

Mark S. Gordon*

Department of Chemistry, Iowa State University, Ames, Iowa 50011-2030

Received: November 30, 2004; In Final Form: March 31, 2005

In an attempt to explore the mechanism for the synthesis of silsesquioxanes (POSS), the entire reaction processes from $HSi(OH)_3$ to T_8, one of the most common and stable POSS was investigated with electronic structure theory calculations, including electron correlation effects. In addition, the effect of some controlling factors, which play important roles in the reaction mechanism, is discussed.

Introduction

Polyhedral oligomeric silsesquioxanes (POSS), $[RSiO_{1.5}]_n$ (n = 4, 6, 8, 10, 12, ...), have attracted considerable experimental and theoretical interest for many years because of their wide variety of practical uses.[1,2] However, most previous studies have focused on the structures and properties of POSS compounds or on modeling surface reactions of silica or zeolites, and the mechanism(s) for the synthesis of POSS is not yet well-understood.

Continuing the present series of electronic structure studies on POSS, we report here the results of calculations on the latter stages of the mechanism for the synthesis of POSS. Previous papers in this series have presented results on the early stages of the reaction mechanism[3a] (hydrolysis and initial condensation) as well as the further condensation to form cyclosiloxanes.[3b] Also investigated have been the effects of substituents such as CH_3, *i*-Pr, *t*-Bu, and phenyl groups, as well as catalytic and solvent waters, on steps of the mechanism.[3c] The present work examines the entire process from $HSi(OH)_3$ to T_8 that is one of the most common and stable POSS species. Of course, there exist many possible pathways. The focus here, for simplicity, is on selected direct pathways that seem the most plausible. In addition, the key factors that determine the reaction mechanisms for the POSS synthesis are explored.

Computational Methods

The geometries of all molecules of interest have been fully optimized by employing the B3LYP hybrid density functional theory[4] using the 6-31G(d) basis set.[5] All compounds were characterized as minima or transition states by calculating and diagonalizing the B3LYP/6-31G(d) Hessian matrix of energy second derivatives. Finally, single-point MP2[6] energy calculations have been performed at all stationary points to obtain more reliable energetics. All relative energies reported in this work have been corrected for harmonic zero-point vibrational energies.[7] All calculations were performed with the GAMESS[8] and Gaussian electronic structure codes.[9]

Result and Discussion

1. Reaction Intermediates. T_8 ($[RSiO_{1.5}]_8$, R = H) is one of the most common and most stable POSS with a cubic structure. Presented here are the most simple, plausible direct routes from the starting molecule, trisilanol ($HSi(OH)_3$), to the desired product T_8. The entire reaction scheme, including all intermediates considered, is shown in Figure 1. Previous papers in this series have investigated the reaction mechanisms of hydrolysis to form $HSi(OH)_3$ from trihalosilane ($RSiX_3$) and the subsequent condensations to form disiloxane ($H(OH)_2SiOSi(OH)_2H$)[3a] and some ring structures, such as cyclosiloxanes ($(H(OH)SiO)_n$, n = 3, 4).[3b] Therefore, the focus in the present

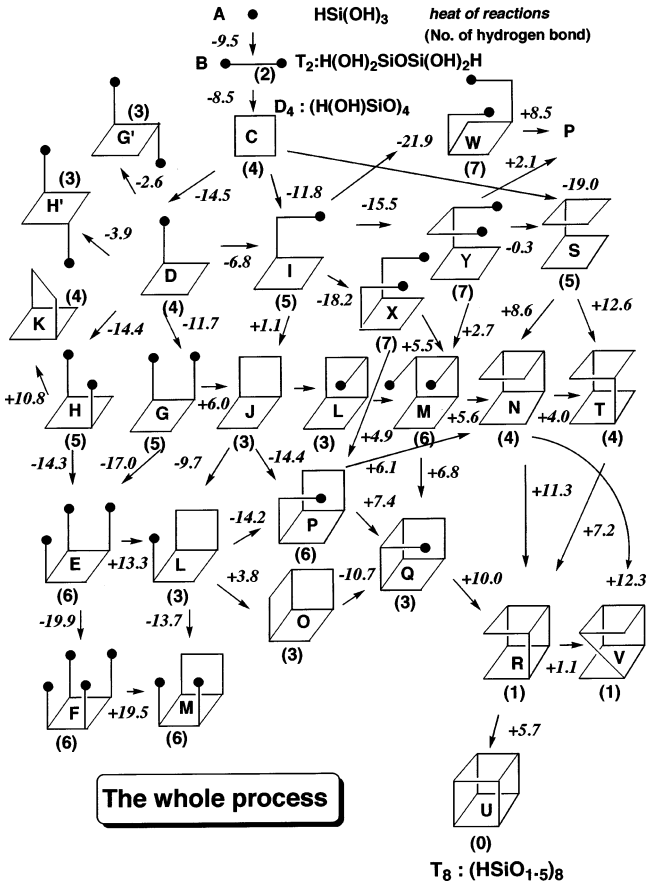

Figure 1. Schematic of all processes from silanol (**A**; $HSi(OH)_3$) to T_8 (**U**). The numbers are the MP2//B3LYP/6-31G(d) + ZPC reaction energies along the direction of the arrow. Numbers in parentheses are the number of intramolecular hydrogen bonds that are shorter than 2.5 Å.

10.1021/jp040731b CCC: $30.25
Published on Web 05/25/2005

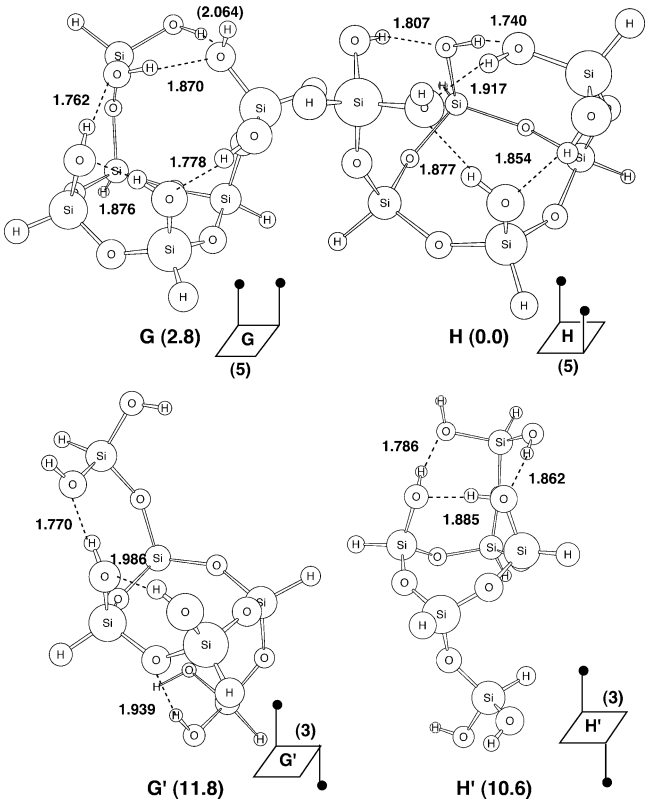

Figure 2. B3LYP/6-31G(d) optimized structures of **G**, **G′**, **H**, and **H′** in angstroms. The MP2//B3LYP/6-31G(d) + ZPC energies relative to **H** are in parentheses.

work is on the further condensations from D_4 ($(H(OH)SiO)_4$) to produce T_8. In addition, a key aspect of this investigation is to obtain a fundamental understanding of the most important factors that control the reaction mechanisms.

Before discussing the mechanisms in detail, it is worthwhile to examine the structure and the stability of some reaction intermediates, often referred to as incompletely condensed POSS. This means these structures still have one or more OH groups that may still participate in further condensations. Therefore, these species have some intramolecular hydrogen bonds through the remaining OH groups, as indicated in Figure 1. In general, one expects that the existence of hydrogen bonds via the OH groups should make the intermediate more stable compared to other isomers that do not have hydrogen bonds.

First, compare structures **G** and **H** and their trans isomers **G′** and **H′** (Figure 2), where trans refers to the relative orientation of the dihydroxysilanyl groups. Although it is clear that the trans isomers do not play a central role as intermediate complexes in a direct mechanism that leads to T_8, these isomers are considered in order to obtain a thorough understanding of the overall mechanism and competing processes. As the figure shows, the number of hydrogen bonds is smaller in the trans isomers (**G′** and **H′**) than in the corresponding cis isomers (**G** and **H**). This stabilization due to hydrogen bonding results in the preferential formation of cage structures leading ultimately to T_8 in a stepwise manner.

Next, consider the location where an additional Si unit attaches in a stepwise manner. The two Si units (small black circles in the figure) are adjacent to each other in **G** and **G′**, while they are diagonally displaced in **H** and **H′**. The number of hydrogen bonds is the same in both cis isomers (**G** and **H**) and in both trans isomers (**G′** and **H′**); however, the isomers with the diagonal arrangement (**H** and **H′**) are more stable than

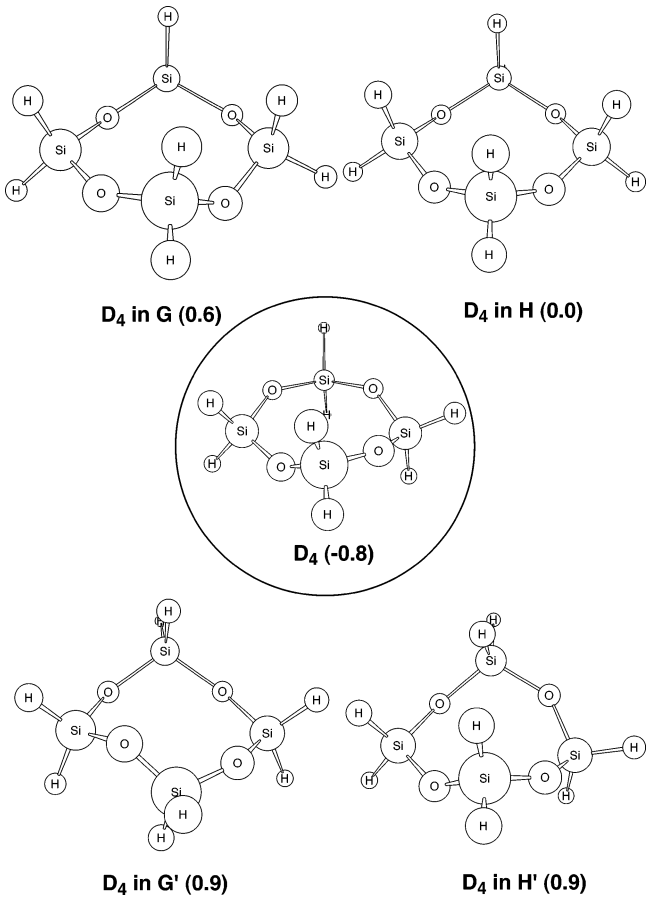

Figure 3. B3LYP/6-31G(d) optimized structures of $(H_2SiO)_4$ where the framework of the ring is fixed as in the intermediates. The $(H_2SiO)_4$ in the center is the fully optimized structure at the same level of theory. The energies relative to cyclotetrasiloxane with the framework of **H** at the same level of theory are in parentheses.

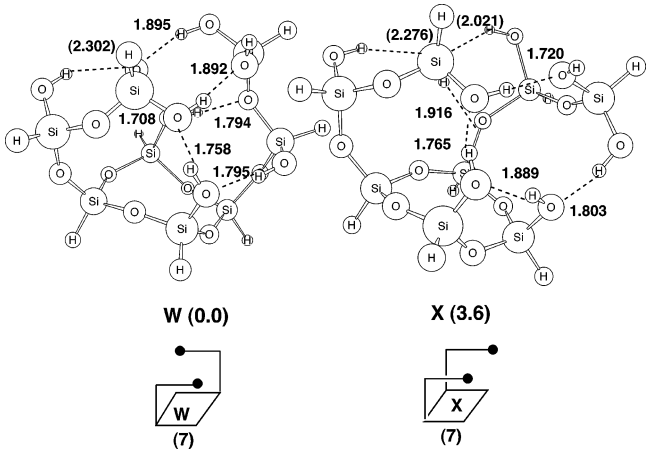

Figure 4. B3LYP/6-31G(d) optimized structures of **W** and **X** in angstroms. MP2//B3LYP/6-31G(d)+ZPC energies relative to **W** are in parentheses.

those with adjacent groups (**G** and **G′**). This is probably a steric effect. As a result, the D_4 plane may be deformed significantly in **G** and **G′**. To confirm this, compare the stability of the D_4 plane in the four isomers. Figure 3 shows $(H_2SiO)_4$ obtained by full geometry optimization, except that the D_4 frameworks (dihedral angles) are fixed at the values in the four isomers.[10] Fully optimized $(H_2SiO)_4$ is also shown in the center of the figure for comparison. The energy differences are very small, but the order of stability is the same as in the four isomers, **G**, **G′**, **H**, and **H′**.

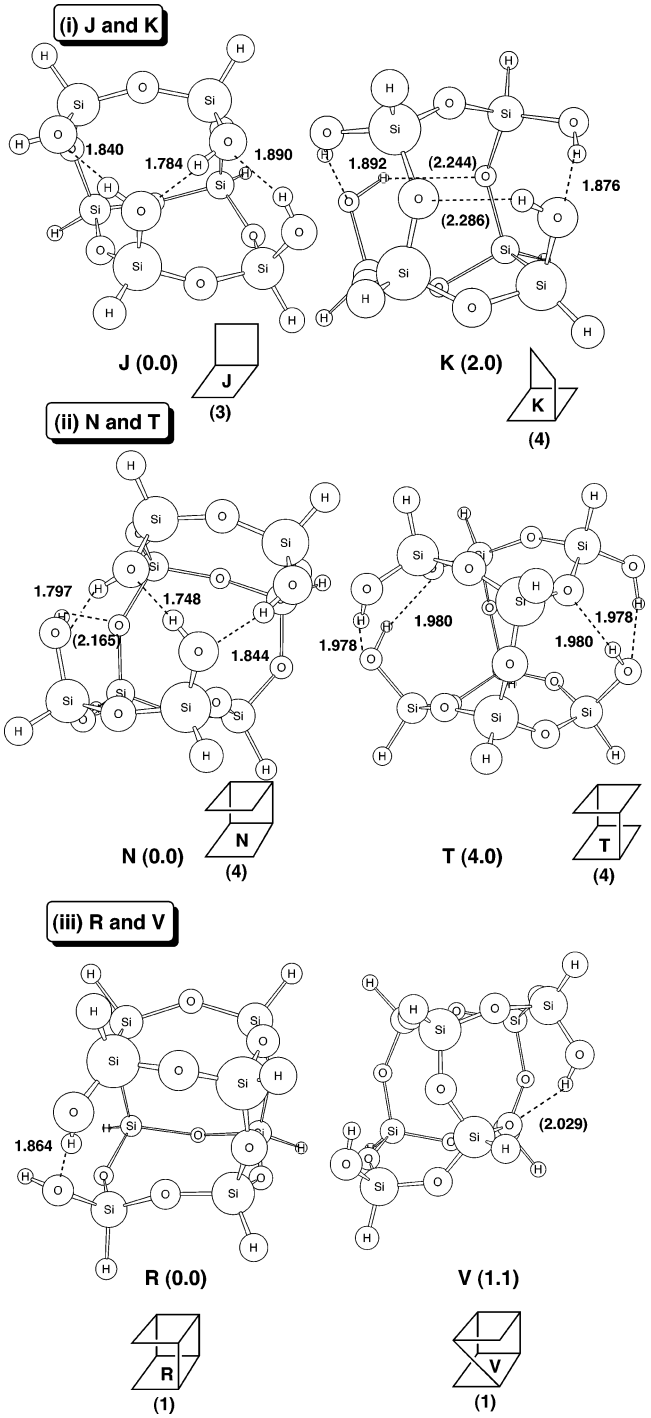

Figure 5. B3LYP/6-31G(d) optimized structures of (i) **J** and **K**, (ii) **N** and **T**, and (iii) **R** and **V** in angstroms. MP2//B3LYP/6-31G(d) + ZPC energies relative to **J**, **N**, and **R** are in parentheses.

Similar considerations apply to the species **W** and **X** as shown in Figure 4. In **W**, two Si_2 (disiloxane) units are attached diagonally to each other in the D_4 ring, while these units are in adjacent positions in **X**. The two isomers have the same number of hydrogen bonds, although these bonds are shorter, and therefore probably stronger, in **W**. The $(H_2SiO)_4$ unit in D_4 in **W** is slightly more stable than that in **X**, by 0.6 kcal/mol.[11] Even though these energy differences are small, it appears that the additional stepwise condensation on D_4 may take place preferentially in such a manner as to reduce steric crowding. This effect is expected to become more important when bulky substituents are present.

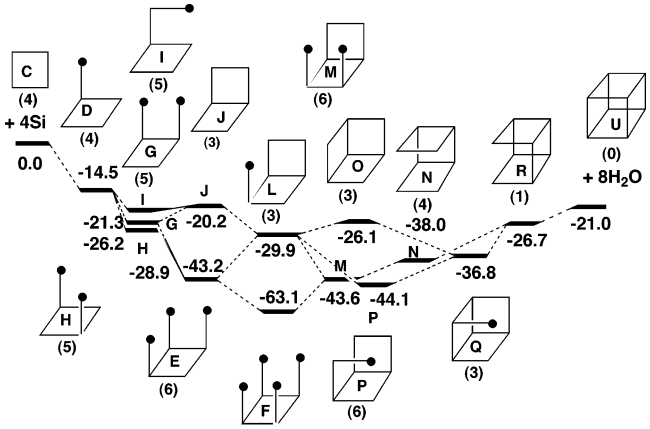

Figure 6. MP2//B3LYP/6-31G(d) + ZPC reaction energies from **C** to **U** in mechanism (i).

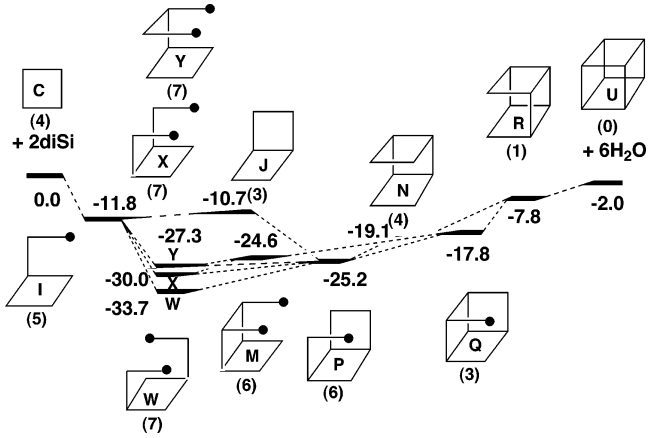

Figure 7. MP2//B3LYP/6-31G(d) + ZPC reaction energies from **C** to **U** in mechanism (ii).

Next, consider the three pairs of isomers, (i) **J** and **K**, (ii) **N** and **T**, and (iii) **R** and **V** in Figure 5. These species correspond to the next sequence of steps in the ultimate synthesis of T_8. In **J** and **K**, a second D_4 unit has been built as a second face of a cube (**J**) or as a diagonal face (**K**). The structure with the stronger hydrogen bonds (**J**) is lower in energy by 2 kcal/mol. **N** and **T** build another D_4 plane upon **J**, again as a new face in the ultimate cube (**N**) or as a diagonal plane (**T**). Once again, the former structure with stronger hydrogen bonds is lower in energy by 4 kcal/mol. Structures **R** and **V** follow the same pattern. In all cases, the number of *efficient* hydrogen bonds rather than only the number seems to be important in determining the relative stability of intermediate structures. In addition, the formation of the deformed larger rings in **K** (D_5), **T** (D_6), and **V** (D_5) may contribute to the instability of these structures.

2. Heats of Reaction for the Three Types of Condensation. As illustrated in Figure 1, there are many possible intermediate complexes, and they have been divided into three types of condensation from **C** (D_4), namely condensations that proceed by (a) successive additions of a trisilanol unit (denoted Si) (the corner addition mechanism), (b) additions of two Si (disiloxane) units (denoted diSi) (edge addition mechanism) and (c) a D_4 plane (plane addition mechanism). Hybrid mechanisms (mixtures of two or three types) may be also possible, but these have not been considered in this study. The relative energies for these three processes are displayed in Figures 6−8, respectively. The corner addition mechanism (type (a)) begins with the addition of one trisilanol (Si) unit to **C** to form the first intermediate **D**. Successive Si additions lead to **H** (or **G**)

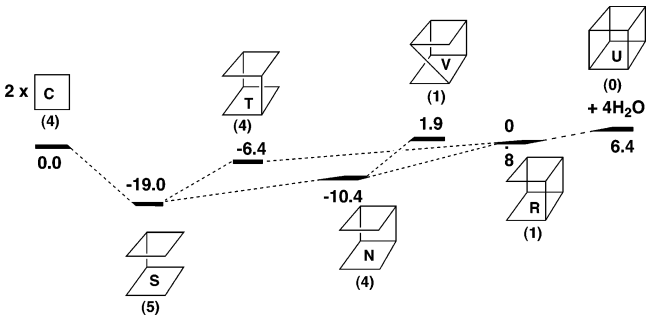

Figure 8. MP2//B3LYP/6-31G(d) + ZPC reaction energies from **C** to **U** in mechanism (iii).

→ **E** → **F** (with eight Si units). Routes to other structures with eight Si units (e.g., **M** or **P**) proceed via the intermediate **L**; for example, **H** (or **G**) → **E** → **L** → **M** or **H** (**G**) → **E** → **L** → **P**. The heat of reaction increases when a D_4 plane is formed at **L**, probably because of ring strain. This is always seen for the corresponding reactions considered here. However, the heat of reaction decreases at **L** if the mechanism proceeds through intermediate **J**; **G** → **J** → **L** or **I** → **J** → **L**. **L** may be considered to be the direct precursor of **O.** This process **E** → **O** is endothermic. Because **O** can be a starting material for the synthesis of various new functional POSS compounds,[2h] it has been investigated frequently and recently detected experimentally.[2j]

The intermediate complex on this section of the potential energy surface with the lowest energy compared to **C** is **F**; **F** + 4 H_2O lies 63.1 kcal/mol below **C** + 4 **A**. After the intermediates with eight Si units are formed, the remaining steps that lead to the final T_8 product **U** are *net* endothermic, although some individual steps correspond to energy decreases. The final product, **U** (T_8), is 21.1 kcal/mol lower in energy than **C** plus four Si units, so that the overall process in this mechanism is exothermic.

For the edge addition mechanism (b) in Figure 7, the initial step is the addition of a diSi unit to form the intermediate **I**. Then, the structure with eight Si units (**W**, **X**, or **Y**) is formed by the addition of one more disiloxane. **W** is the most stable of these three intermediates. **W** + 2 H_2O lies 33.7 kcal/mol lower than **C** + 2 **B**. Condensation then proceeds from **W** (or **X** or **Y**) → **P** → **Q** or **X** (or **Y**) → **M** → **N,** with an accompanying increase in energy. **N** or **Q** can then proceed to **R** and then finally to **U**. A similar energy increase was found for mechanism (a) in Figure 6. As for mechanism (a), mechanism (b) is also net exothermic relative to starting reactants **C** plus two diSi units. However, the exothermicity is only 2.0 kcal/mol, as compared with ∼21 kcal/mol for mechanism (a).

Mechanism (c), illustrated in Figure 8, is quite simple. **S** (the structure with eight Si units) is first formed by the condensation of two D_4 planes. This reaction is 19.0 kcal/mol exothermic. All subsequent steps are endothermic condensations, and the net reaction 2 **C** → **U** + 4 H_2O is endothermic by 6.4 kcal/mol. This mildly endothermic process is the most direct route to T_8 among the three mechanisms.

These purely thermodynamic comparisons suggest that, *in the gas phase*, mechanism (a) is strongly exothermic, mechanism (b) is slightly exothermic, and mechanism (c) is slightly endothermic. Except for the final step in mechanism (c), all intermediates in all mechanisms lie lower in energy than the starting reactants. So, all three mechanisms are *thermodynamically* feasible. Despite the fact that low-lying intermediates exist in all three mechanisms (e.g., **F** in mechanism (a), **W** in mechanism (b), **S** in mechanism (c)), sufficient energy is available in the first two mechanisms to drive the reaction to products. However, the next step is to consider the barrier heights for each reaction, to determine the kinetic effects on the three competing mechanisms.

3. Condensation Barriers. Therefore, we now consider the transition structures for the condensation reactions in all three mechanisms. The first three reactions to be discussed are (i) **C** + **A** → **D** (Figure 6), (ii) **C** + **B** → **I** (Figure 7), and (iii) **C** + **C** → **S** (Figure 8), plus the appropriate number of extruded water molecules in each case. There are two types of transition structures (**TS1** and **TS2**) for the first two reactions, as shown in Figure 9. In both reactions (i) and (ii), the leaving water is formed from an H of the D_4 moiety and a silanol or disiloxane OH group in **TS1**, while in **TS2**, the OH of D_4 abstracts an H from a silanol or disiloxane. D_4 has an all-cis conformation,[3b] as shown in the center of the figure, because of the hydrogen bond network. Note that the D_4 structure is not very deformed in **TS1**, whereas in **TS2**, the D_4 moiety is much more deformed. This may be why **TS1** is more stable than **TS2** in both

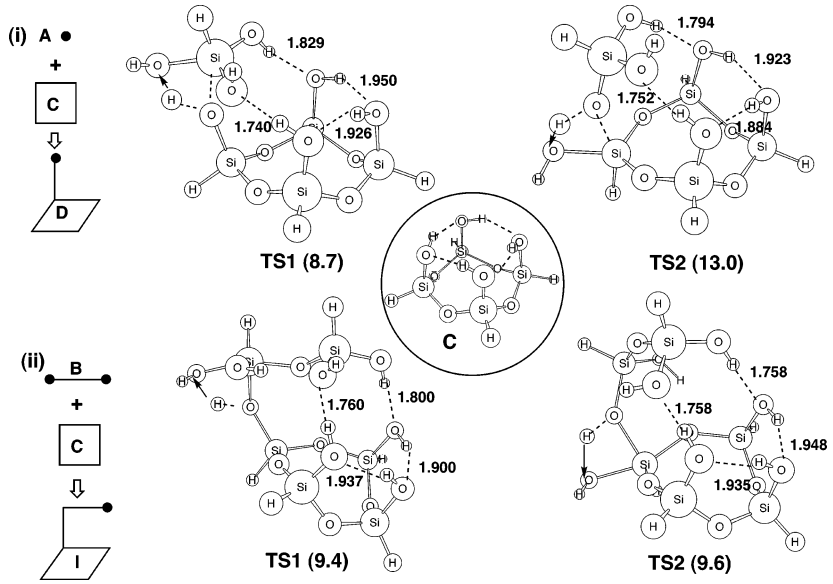

Figure 9. Two types of B3LYP/6-31G(d) transition structures for the reactions (i) **C** + **A** → **D** and (ii) **C** + **B** → **I**. The MP2//B3LYP/6-31G(d) + ZPC energies relative to the reactants are in parentheses.

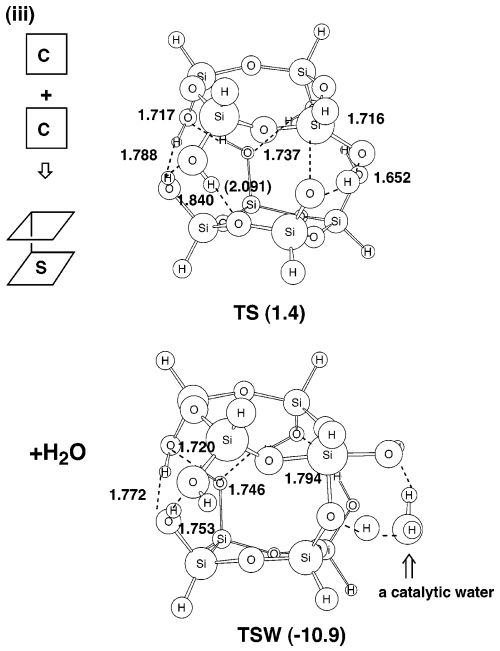

Figure 10. B3LYP/6-31G(d) transition structure for **C** + **C** → **S** (upper) and with a catalytic water (lower) in angstroms. MP2//B3LYP/6-31G(d) + ZPC energies relative to the reactants are in parentheses.

mechanisms. The energy difference between the alternative transition states is only ~1 kcal/mol for reaction (ii), but it is more than 4 kcal/mol for reaction (i). Interestingly, there are four hydrogen bonds in both **TS1** and **TS2** for both reactions. The **TS1** energy barrier is slightly (<1 kcal/mol) lower for reaction (i) than for reaction (ii).

For reaction (iii), only one transition structure has been located, as shown in Figure 10. This transition state has many hydrogen bonds, thereby making it much lower in energy than the most favorable (**TS1**) transition states in reactions (i) and (ii), with a barrier height of just over 1 kcal/mol. Therefore, this D_4-D_4 condensation is predicted to take place very easily even in the gas phase. In previous studies in this series, it has been shown that water can function as a very effective catalyst. Addition of just one water molecule can dramatically lower barrier heights to about zero or nearly so.[3a-c] The addition of observer waters lowers the barrier even further. Because the transition state in Figure 10 is the lowest in energy among the mechanisms studied here, the impact of one water molecule was analyzed, leading to transition structure **TSW** in Figure 10. As in the earlier studies, this leads to a zero barrier for this reaction.

Because the first step in reaction (iii) is energetically favored (because of the large number of hydrogen bonds) relative to the first steps of reactions (i) and (ii), it is sensible to explore the transition structures and associated barrier heights for the subsequent steps in this mechanism. It is important to note, however, that on the basis of previous studies of condensation reactions, the addition of water molecules will also greatly reduce the barriers for the first steps of mechanisms (a) and (b) as well. This will be explored in a later work. The remainder of this work focuses on mechanism (c).

4. Mechanism (c). The final stage of the present study is to complete the potential energy surface for mechanism (c), by locating transition structures that connect the intermediates. As may be seen in Figure 8, once **S** has been formed, all subsequent condensations correspond to formation of new edges, because **S** already contains the full complement of 8 Si units. So, each subsequent reaction is endothermic until the final product **U** (T_8) has been formed. Figure 11 presents a schematic of the potential energy surface from **A** to **U**. It is important to note that, in this figure, all product waters are implied, and each barrier refers to the energy required to form the corresponding intermediate, while each heat of reaction is for 1 mol of the corresponding product. The barrier heights for these successive condensation reactions are relatively high except for the first reaction (**C** → **S**), as mentioned before. Especially, the barrier heights for the reactions **V** → **R** and **R** → **U** are found to be large. The transition structures for the reactions **V** → **R** and **R** → **U** are shown in Figure 12. The former process is a bond alternation reaction caused by a hydrogen atom exchange between two oxygen atoms in the transition structure. Interestingly, according to experimental observations, **V**, but not **R**, is observed and isolated in the synthesis of **U** ($[MeSiO_{1.5}]_8$ in the experiment).[12] These two isomers are predicted here to be comparable in energy, and **V** has the largest barrier separating it from the final product. This may explain why it is observed. Because the direct isomerization from **R** to **U** is also predicted to involve a sizable barrier, one could speculate that **R** might also be isolable. However, the transition structure for the condensation from **R** to **U** has the usual four-centered structure for the active site. So, this transition state may be stabilized by the addition of water. To confirm this, the transition states with a catalytic water were also located; they are shown in Figure 12. Both transition states have six-centered structures, and the energy barriers are significantly reduced (see Figure 11) as expected. This has also been observed in the hydrolysis and the early stages of condensation reactions **A** → **B** and **B** → **C**.

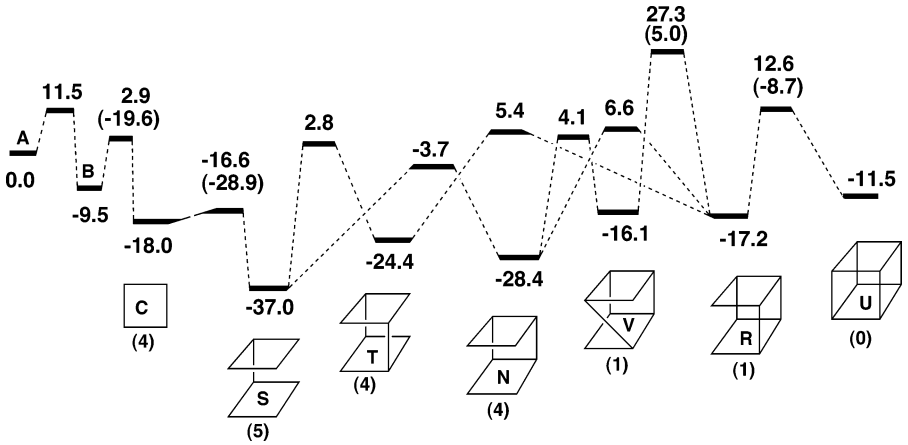

Figure 11. MP2//B3LYP/6-31G(d) + ZPC potential energy surface for the reaction from **A** to **U** in mechanism (iii). The energies are given relative to **A**. In parentheses are the energy barriers in the presence of a catalytic water.

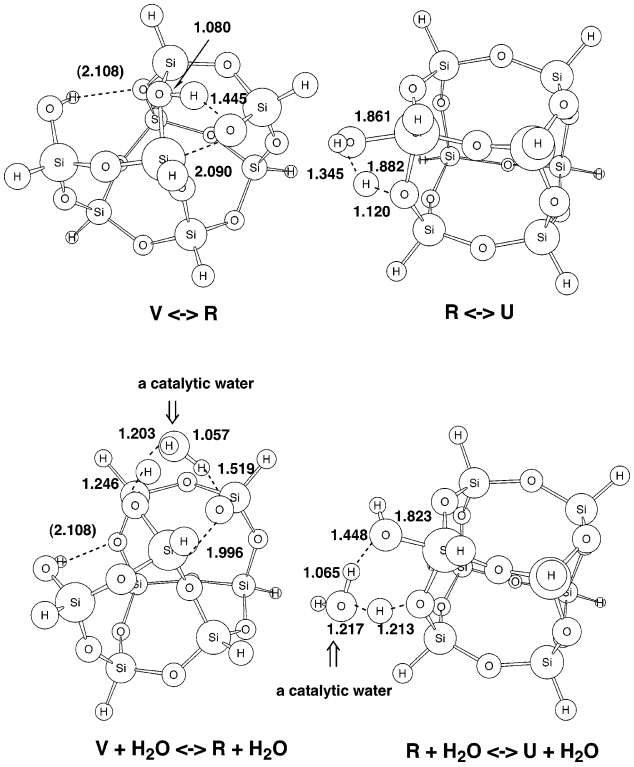

Figure 12. Transition structures for the reactions **V** ↔ **R** and **R** ↔ **U** (upper) and with a catalytic water (lower) at the B3LYP/6-31G(d) level in angstroms.

Furthermore, the overall reaction, starting from **A**, is exothermic by 11.5 kcal/mol, suggesting that the formation of T_8 from A is relatively easy in water solvent.

Concluding Remarks

In an attempt to explore the entire mechanism from silanol to T_8, a large number of intermediates and transition structures on several pathways have been located. It is found that the heat of reaction decreases as the number of Si units increases, while it increases as the number of edges (of the cubic structure) or planes increases. Hydrogen bonds play a very important role in the relative stabilities of intermediates and transition structures and reaction mechanisms as a result. In addition, the deformation of the D_4 ring seems to have an important effect.

Among the three types of mechanisms from D_4 to T_8 considered here, the plane addition condensation is found to be the energetically most favorable, although the energy barrier for each process is relatively high in the gas phase. The overall reaction, starting from **A**, is exothermic by 11.5 kcal/mol. Furthermore, one catalytic water is expected to reduce the barrier, as seen in the early stages of condensation or hydrolysis in our previous studies. Of course, there may be many other mechanisms (involving ring expansion in D_3 or T_6, for example) that have not been considered here. These alternative mechanisms will be considered in later work. In addition, it is likely that the effect of substituents on the silicon atoms may be very important for all of the reaction mechanisms. Analyses of substituent effects are also in progress.

Acknowledgment. The authors are grateful to Dr. Maki Itoh for informative discussions. This work has been supported by the Air Force Office of Scientific Research (M.S.G.). Computer time has been made available via a Grand Challenge grant from the DOD High Performance Computing Modernization Office on the T3E computers at ERDC and AHPCRC and a grant from the Research Center for Computational Science (Okazaki, Japan).

References and Notes

(1) As the reviews, for example, (a) Voronkov, M. G.; Lavrent'yev, V. L. *Top. Curr. Chem.* **1982**, *102*, 199. (b) Feher, F. J.; Newman, D. A.; Walzer, J. F. *J. Am. Chem. Soc*. **1989**, *1111*, 1741. (c) Baney, R. H.; Itoh, M.; Sakakibara, A.; Suzuki, T. *Chem. Rev*. **1995**, *95*, 1409. (d) Feher, F. J.; Budzichowski, T. A. *Polyhedron* **1995**, *14*, 3239.

(2) As the recent paper, for example, (a) Skowronska-Ptasinska, M. D.; Duchateau, R.; van Santen, R. A.; Yap, G. P. A. *Organometallics* **2001**, *20*, 3519. (b) Lorenz, V.; Spoida, M.; Fischer, A.; Edelmann, F. T. *J. Organomet. Chem*. **2001**, *625*, 1. (c) Itoh, M. *Keiso Kagaku Kyoukaishi* **2001**, *15*, 19. (d) Kudo, T.; Gordon, M. S. *J. Phys. Chem. A* **2001**, *105*, 11276. (e) Baudilio, T.; Gordon, M. S. *J. Phys. Chem. B* **2002**, *106*, 11764. (f) Bassindale, A. R.; Liu, Z.; MacKinnon, I. A.; Taylor, P. G.; Yang, Y.; Light, M. E.; Horton, P. N.; Hursthouse, M. B. *J. Chem. Soc., Dalton Trans.* **2003**, 2945. (g) Bassindale, A. R.; Parker, D. J.; Taylor, P. G.; Watt, A. C. *Can. J. Chem.* **2003**, *81*, 1341. (h) Van der Vlugt, J. I.; Fioroni, M.; Ackerstaff, J.; Hanssen, R. W. J. M.; Mills, A. M.; Spek, A. L.; Meetsma, A.; Abbenhuis, H. C. L.; Vogt, D. *Organometallics* **2003**, *22*, 5297. (i) Bassindale, A. R.; Liu, Z.; Parker, D. J.; Taylor, P. G.; Horton, P. N.; Hursthouse, M. B.; Light, M. E. *J. Organomet. Chem.* **2003**, *687*, 1. (j) Pescarmona, P. P.; Raimondi, M. E.; Tetteh, J.; McKay, B.; Maschmeyer, T. *J. Phys. Chem. A* **2003**, *107*, 8885. (k) Kudo, T.; Gordon, M. S. *J. Phys. Chem. A* **2003**, *107*, 8756. (l) Haxton, K. J.; Cole-Hamilton, D. J.; Morris, R. E. *J. Chem. Soc., Dalton Trans.* **2004**, 1665. (m) Dare, E. O.; Olatunji, G. A.; Ogunniyi, D. S. *J. Appl. Polym. Sci.* **2004**, *93*, 907. (n) Liu, L.-K.; Dare, E. O. *J. Chin. Chem. Soc*. **2004**, *51*, 175. (o) Pescarmona, P. P.; Van der Waal, J. C.; Maschmeyer, T. *Chem.—Eur. J.* **2004**, *10*, 1657. (p) Choi, J.; Yee, A. F.; Laine, R. M. *Macromolecules* **2004**, *37*, 3267.

(3) (a) Kudo, T.; Gordon, M. S. *J. Am. Chem. Soc*. **1998**, *120*, 11432. (b) Kudo, T.; Gordon, M. S. *J. Phys. Chem. A* **2000**, *104*, 4058. (c) Kudo, T.; Gordon, M. S. *J. Phys. Chem. A* **2002**, *106*, 11347.

(4) (a) Lee, C.; Yang, W.; Parr, R. G. *Phys. Rev*. **1988**, *B37*, 785. (b) Miehlich, B.; Savin, A.; Stoll, H.; Preuss, H. *Chem. Phys. Lett*. **1989**, *157*, 200. (c) Becke, A. D. *J. Phys. Chem*. **1993**, *98*, 5648.

(5) (a) Hehre, W. J.; Ditchfield, R.; Pople, J. A. *J. Phys. Chem*. **1972**, *56*, 2257. (b) Francl, M. M.; Pietro, W. J.; Hehre, W. J.; Binkley, J. S.; Gordon, M. S.; Defrees. D. J.; Pople, J. A. *J. Chem. Phys*. **1982**, *77*, 3654. (c) Clark, T.; Chandrasekhar, J.; Spitznagel, G. W.; Schleyer, P. v. R. *J. Comput. Chem*. **1983**, *4*, 294. (d) Frisch, M. J.; Pople, J. A.; Binkley, J. S. *J. Chem. Phys*. **1984**, *80*, 3265. (e) Okuno, Y. J. *Chem. Phys*. **1996**, *105*, 5817, and references therein.

(6) Pople, J. A.; Seeger, R.; Krishnann, R. *Int. J. Quantum Chem*. **1979**, *S11*, 149.

(7) We did not calculate the entropies and free energies, because the compounds of interest here have many low-frequency, large-amplitude modes, such as Si−O−Si bends. Therefore, using the harmonic approximation to predict entropies results in very large errors. Consequently, only enthalpy differences are reported here. See (a) Strajbl, M.; Florian, J.; Warshel, A. *J. Am. Chem. Soc*. **2000**, *122*, 5354. (b) Strajbl, M.; Florian, J.; Warshel, A. *J. Phys. Chem.* **2001**, *B105*, 4471. (c) Njegic, B.; Gordon, M. S. Manuscript in preparation.

(8) Schmidt, M. W.; Baldridge, K. K.; Boatz, J. A.; Elbert, S. T.; Gordon, M. S.; Jensen, J. H.; Koseki, S.; Matsunaga, N.; Nguyen, K. A.; Su, S.; Windus, T. L.; Dupuis, M.; Montgomery, J. A., Jr. *J. Comput. Chem.* **1993**, *14*, 1347.

(9) Frisch, M. J.; Trucks, G. W.; Schlegel, H. B.; Gill, P. M. W.; Johnson, B. G.; Robb, M. A.; Cheeseman, J. R.; Keith, T.; Petersson, G. A.; Montgomery, J. A.; Raghavachari, K.; Al-Laham, M. A.; Zakrzewski, V. G.; Ortiz, J. V.; Foresman, J. B.; Cioslowski, J.; Stefanov, B. B.; Nanayakkara, A.; Challacombe, M.; Peng, C. Y.; Ayala, P. Y.; Chen, W.; Wong, M. W.; Andres, J. L.; Replogle, E. S.; Gomperts, R.; Martin, R. L.; Fox, D. J.; Binkley, J. S.; Defrees, D. J.; Baker, J.; Stewart, J. P.; Head-Gordon, M.; Gonzalez, C.; Pople, J. A. *Gaussian 94*; Gaussian, Inc.: Pittsburgh, PA, 1995.

(10) The reason for using $(H_2SiO)_4$ instead of $(H(OH)SiO)_4$ is the hydrogen bonds made among the four OH groups in the latter prevent the isolation of the effect of the deformation of the plane. The B3LYP/6-31G(d) energy (au) of $(H_2SiO)_4$ is as follows: −1464.022 88 (fully optimized), −1464.020 61 (in **G**), −1464.020 27 (in **G′**), −1464.021 65 (in H), and −1464.020 16 (in **H′**), respectively.

(11) The B3LYP/6-31G(d) energy (au) of $(H_2SiO)_4$ is −1464.021 68 (in **W**) and −1464.020 79 (in **X**), respectively.

(12) (a) Kondo, T.; Yoshii, K.; Horie, K.; Itoh, M. *Macromolecules* **2000**, *33*, 3650. (b) Itoh, M. Silsesquioxanes—Potential Building Blocks for Organic−Inorganic Hybrids. In *Conversation between Polymer Science and Inorganic Chemistry*, SPSJ ed.; NTS: Tokyo, 2001.